Microwave absorption in the cores of Abrikosov vortices pinned by artificial insulator inclusion

B. Rosenstein,[1,2] I. Shapiro,[3] E. Deutch,[3] and B. Ya. Shapiro[3]
[1]*Department of Electrophysics and NCTS, National Chiao Tung University, Hsinchu, Taiwan, Republic of China*
[2]*Applied Physics Department, Ariel University Center of Samaria, Ariel 40700, Israel*
[3]*Department of Physics, Institute of Superconductivity, Bar-Ilan University, Ramat-Gan 52900, Israel*
(Received 28 June 2011; published 17 October 2011)

The spectrum of core excitations of the Abrikosov vortex pinned by a dielectric inclusion or nanoholes the size of the coherence length is considered using the Bogoliubov-deGennes equations beyond the semiclassical approximation. While the lowest excitation, minigap, in the unpinned (or pinned by a metallic defect) vortex is of the order of Δ^2/E_F, it becomes of the order of the superconducting gap Δ (E_F is Fermi energy). The reconstruction of the quasiparticle excitations' spectrum has a significant impact on optical properties and on the tunneling density of states. We calculate the absorption amplitude and point out that, while in scanning tunneling microscopy the energy gap $\Delta_{\rm DOS}$ is between a quasiparticle state with angular momentum $\mu^e = \mu_0 > 1/2$ and quasihole with $\mu^h = -\mu_0$, the microwave absorption gap, $\Delta_{\rm dir}$, is between the states with $\mu^e = \mu^h \pm 1$. It is shown that $\Delta_{\rm dir} > \Delta_{\rm DOS}$. The large minigap might play a role in magneto-transport phenomena broadly associated with the "superconductor-insulator" transition in quasi-two-dimensional systems in which small insulating inclusions are generally present.

DOI: 10.1103/PhysRevB.84.134521 PACS number(s): 74.25.N−, 74.25.Wx, 74.25.Gz

I. INTRODUCTION

A distinctive remarkable feature of a superconducting state, a quantum mechanical macroscopic coherent state, is its rigidity.[1] This robust rigidity (even a certain amount of nonmagnetic impurities does not spoil this feature due to the Anderson theorem) leads to the absence of dissipation. This is a result of the energy gap Δ (of the order of $k_B T_c$) in the spectrum of excitations of the many-body system around the Fermi level observed early on both in measurements of microwave absorption[2] (even before its BCS theory[3]) and of tunneling density of states[4] (DOS).

Unfortunately, the magnetic field always destroys this property. In type II superconductors it creates Abrikosov vortices with cores of radius ξ (coherence length), in the center of which the superfluid density vanishes due to a nonzero vorticity.[5] This feature is of topological nature and therefore unavoidable. In the vortex core center the material resembles a normal metal in the sense that the spectrum of the fermion excitations is almost continuous. In fact, the spectrum is discrete since the charge $\pm e$ quasiparticles are "confined" by Andreev reflection inside the vortex core with typically small interlevel spacing and the minimal excitation (the minigap in DOS) $\Delta_{\rm DOS}$ of the same order. Theoretically the core excitation spectrum of unpinned vortices in clean *s*-wave superconductors was calculated a long time ago[6,9] using the Bogoliubov-deGennes equations (BdG). It is linear, $E_\mu = \mu\Delta^2/E_F$, as a function of the half-integer angular momentum $\mu = 1/2, 3/2, \ldots$. Therefore the minimal excitation, $\Delta_{\rm DOS} = \Delta^2/E_F$, occurs at the smallest possible angular momentum $\mu_0 = 1/2$ and is much smaller than Δ. The calculation (valid for not very large μ and zero temperature) was later improved (in particular, made self-consistent[10,11]) and generalized in various directions to include higher angular momenta, *d*-wave pairing[12] and vortex line curvature.[11]

The influence of the core excitations (Andreev bound states) on local DOS was first observed in the clean superconductor $NbSe_2$ using scanning tunneling spectroscopy (STM).[13] Recent developments of the STM technique allow identification of the core states in a wide variety of materials.[14] The core excitations lead to dissipation when the vortices move or vibrate. The dynamics of the vortex motion, very important for applications,[5] depends therefore essentially on the excitation spectrum of the vortex core.

The above theories considered unpinned vortices although vortices are seldom free in real superconductors. Usually they are weakly pinned by spatial inhomogeneities. It is expected that the spectrum of a vortex pinned on metallic defects is not modified significantly due to the proximity effect. However, in addition to inhomogeneities, superconducting material can also tolerate small insulating inclusions and even holes. In fact, an early method to ensure pinning of vortices was irradiation that creates such an insulating columnar defect.[15] Recently a more efficient method, the ultrafast laser and electron-beam lithography, was realized experimentally in thin films to produce arrays of dielectric inclusions or holes.[16,17] It has an advantage over the randomly distributed intrinsic or columnar defects since the pinning centers can be periodically arranged into an array. An even more important feature of the artificial pinning is that the diameter of the hole can be made of the order of the coherent length.[17] In these cases the effect on the core excitation spectrum might be stronger.

Recently, Melnikov *et al.*[18] initiated the study of the spectrum of quasiparticles of a vortex pinned by columnar defects of a radius smaller than the coherence length using the semiclassical approach developed earlier in Ref. 19. For excitations with a large momentum perpendicular to the magnetic field, $k_\perp$, they found an indication that, even when the radius of the columnar defect is as small as $R = 0.1\xi$, the minigap becomes of the order Δ rather than Δ^2/E_F. More specifically, states with a small impact parameter $b = \mu/k_\perp$ have energy of the order Δ (asymptotically $E(b \to 0) = \Delta$); then at larger angular momentum the energy of the bound state decreases linearly. When the impact parameter approaches R, the energy abruptly decreases (infinite slope) signaling the breakdown of the method at $b = R$. It looks like this

decrease is intercepted (just before the breakdown) by the linear behavior $E(b) = \mu b\Delta/\xi$ characteristic to the unpinned vortex spectrum.[6,9] The excitation energy at the intercept is still larger than $\Delta_{\rm DOS} = \Delta^2/E_F$, however, the minimum is beyond the semiclassical approximation applicability region and one might worry about the quantitative result. Qualitatively this allowed them to conclude that one enhances the minigap by placing an insulator, albeit as thin as the columnar defect. If one was to address the dramatic increase of the minigap experimentally, one had to consider all the values of $k_\perp < k_F$ including the small ones. This necessarily requires calculations beyond the semiclassical approximation.

In the present note we ascertain, by solving the BdG equations numerically, that the artificial pinning by an array of holes changes dramatically the excitation spectrum: While the minigap, that in the spectrum of the unpinned vortex (or captured by a metallic defect) is of order Δ^2/E_F, it becomes of the order Δ. We consider arbitrary values of the in-plane wave vector $k_\perp$ and an arbitrary inclusion radius R for both the quasiparticle branch $E^e(\mu)$ and the quasihole branch, $E^e(\mu)$. The results are in agreement with the semiclassical approximation[18] within its range of applicability. It is emphasized that the lowest Andreev bound state appears at elevated angular momentum $\mu^e = \mu_0 > 1/2$. The reconstruction of the spectrum of the quasiparticle excitations has a most significant impact on the optical properties and the tunneling density of states. While in STM the energy gap is between a quasiparticle state with angular momentum μ_0 and a quasihole with $-\mu_0$, $\Delta_{\rm DOS} = E^e(\mu_0) - E^h(-\mu_0)$, the microwave absorption gap is between the states with $\mu^e = \mu^h \pm 1$, $\Delta_{\rm dir} = E^e(\mu_0) - E^h(\mu_0 \pm 1)$ for circular polarizations. It is shown that generally $\Delta_{\rm dir} > \Delta_{\rm DOS}$. The absorption intensity increases quadratically with $k_\perp$.

II. THE BOGOLIUBOV-DE GENNES EQUATIONS FOR A SINGLE VORTEX

We start with the Bogoliubov-de Gennes equations in the operator matrix form for the BdG "spinor":[5]

$$\begin{pmatrix} \hat{H} & \Delta \\ \Delta^* & -\hat{H}^* \end{pmatrix} \begin{pmatrix} u \\ v \end{pmatrix} = E \begin{pmatrix} u \\ v \end{pmatrix}, \tag{1}$$

where E is the energy of the BdG quasiparticles and

$$\hat{H} = \frac{1}{2m}\mathbf{\Pi}^2 - E_F; \quad \mathbf{\Pi} = -i\hbar\nabla - \frac{e}{c}\mathbf{A}. \tag{2}$$

The single vortex order parameter for a rotational symmetric single vortex, $\Delta = |\Delta(r)|e^{-i\varphi}$, where r,φ are the polar coordinates in the x-y plane. The vector potential $\mathbf{A}$ has only the azimuthal component $A_\varphi(r)$ and in the London gauge consists of the singular part $A^s_\varphi = \hbar c/2er$ and the regular part of the vector potential that can be neglected for the large Ginzburg-Landau parameter[5] $\kappa = \lambda/\xi$.

Using the well-known Ansatz[5] for the excitation amplitude in the form,

$$\begin{pmatrix} u \\ v \end{pmatrix} = \begin{pmatrix} f_+(r)e^{i(\mu-1/2)\varphi} \\ f_-(r)e^{i(\mu+1/2)\varphi} \end{pmatrix} e^{ik_z z}, \tag{3}$$

for the half-integer "angular momentum" μ, and substituting it into Eq. (1), one obtains the following one-dimensional equation for the spinor f:

$$\left[\begin{pmatrix} \gamma H_0 & |\Theta| \\ |\Theta| & -\gamma H_0 \end{pmatrix} - \frac{\gamma\mu}{r^2}\right] \begin{pmatrix} f_+ \\ f_- \end{pmatrix} = E_{\mu,k_z} \begin{pmatrix} f_+ \\ f_- \end{pmatrix}. \tag{4}$$

The operator

$$H_0 = -\frac{1}{r}\frac{\partial}{\partial r}\left(r\frac{\partial}{\partial r}\right) - k_\perp^2 + \frac{\mu^2 + 1/4}{r^2}$$

contains $k_\perp^2 \equiv k_F^2 - k_z^2$. ξ is the unit of length and $\gamma = \mathbf{\Delta}_\infty/4E_F$, $\xi = v_F/\Delta_\infty$. The bulk energy gap, Δ_∞, will be units of energy. In principle, the spatial distribution of the order parameter $\Theta(r) = \Delta(r)/\Delta_\infty$ should be determined self-consistently (see Ref. 11), however, it was shown[9–11] that a simple approximation,

$$\Theta_{\rm free}(r) = \frac{r}{\sqrt{r^2+1}}, \tag{5}$$

provides a sufficiently accurate description of the order parameter for the free (unpinned) vortex. This is consistent with the solution of the Ginzburg-Landau (GL) equations.

The spectrum of the quasiparticles ($E^e_{\mu,k_z} > 0$) of these equations for the unpinned vortex can be simply summarized by an approximate universal formula for positive μ found by Clinton:[7]

$$E^e_{\mu,k_z} = \Theta(\mu/k_\perp). \tag{6}$$

The system possesses the following symmetries. The magnetic field breaks the time-reversal symmetry T, however, the equations are invariant under combined CT: $u \to v^*, v \to -u^*$. Each quasiparticle state is accompanied by a corresponding quasihole state with energy,

$$E^h_{\mu,k_z} = -E^e_{-\mu,k_z}. \tag{7}$$

Note that the sign of the angular momentum is reversed and there is no symmetry between positive and negative angular momentum quasiparticles (holes) since vorticity creates chirality of the core excitations. An additional obvious reflection symmetry is $E_{\mu,k_z} = E_{\mu,-k_z}$. In the presence of the insulator inclusion or hole of the radius R we assume that the order parameter profile, Eq. (5), is still accurate for $r > R$. Therefore there are two regions: the insulator inclusion, $0 \leqslant r < R$, where the BdG wave function is strictly zero and the tail of the vortex order parameter in which the order parameter is suppressed near the insulator and approaches the uniform superconductor value at infinity. To find the BdG excitations localized near the vortex, one has to solve Eq. (4) using boundary conditions for BdG localized at the vortex core wave functions,

$$\begin{pmatrix} f_+ \\ f_- \end{pmatrix}_{r=R} = \begin{pmatrix} f_+ \\ f_- \end{pmatrix}_{r\to\infty} = 0, \tag{8}$$

with the order parameter found self-consistently. In BCS with phonon coupling g one obtains

$$\Delta(r) = g \sum_{E_{\mu,k_\perp} < \hbar\omega_D} u_{\mu,k_\perp} v^*_{\mu,k_\perp} (1 - 2f_F(E_{\mu,k_\perp}/T)), \tag{9}$$

where ω_D is the Debye frequency and f_F is the Fermi-Dirac distribution function. Qualitatively the spectrum consists of

several Andreev bound states and a continuum of states above the gap. If there is no magnetic field; there is continuum only resulting in homogeneous condensate $\Delta(r) = \Delta_\infty$. Under magnetic field, neglecting the quantum effect of emergence of the discrete bound state coming from the continuum, one would obtain the mean-field solution of the GL equations with effective $\xi(T)$ [Eq. (5)]. The effect of bound states is rather small (see Ref. 10), so that the GL spatial distribution of the order parameter is sufficiently precise. In the case of the insulator inclusion the superconductor-insulator (SI) interface is formed. In a microscopic theory of the SI interface (see, e.g., Ref. 8), the order parameter rises abruptly from zero in dielectric (where amplitudes of normal excitations $f_\pm = 0$) to a finite value inside the superconductor within an atomic distance a from the interface, namely with an "infinite" slope $\propto 1/a$. Therefore, as in Ref. 18, we assume a discontinuous distribution:

$$\Theta(r) = \begin{cases} 0 & r < R \\ \frac{r}{\sqrt{r^2+1}} & r > R \end{cases} . \tag{10}$$

The boundary conditions, on the amplitudes $f_\pm$ [Eq. (8)], are consistent with the zero-order parameter at the boundary point $r = R - a$. Next we show that that this set of boundary conditions, even for $R \to 0$, leads to a spectrum different from that in Eq. (6).

III. ANDREEV BOUND STATES SPECTRUM

The BdG equations subject to the insulator inclusion boundary condition [Eq. (8)], were solved numerically for clean superconductors, $\gamma = 2.5 \cdot 10^{-3}$. The radial equation was discretized and the whole spectrum of particle and hole excitation was calculated despite the appearance of oscillations of the order $1/k_F$. This required a very small step (2×10^{-3}) and large size for elevated angular momenta (up to 120; large enough for realistic situations considered below). As a test for the accuracy of the calculation, the threshold at energy Δ_∞ was required to be within 0.1% for both quasiparticles and quasiholes. The results for the positive angular momentum (quasiparticle) branch of the BdG spectrum for $k_\perp = 10, 50, 200$ are presented in Fig. 1 for values of the hole radius $R = 0.4$. As estimated below, the maximal value of $k_\perp^{\max}$ in metals can reach several hundred. The results at small positive angular momenta (corresponding to a small impact parameter $b \approx \mu/k_\perp$) are lower than the semiclassical approximation[18] plotted as purple lines. In this case the wave function is restricted to avoid insulator inclusion. The energy decreases as the angular momentum increases and reaches a minimum at μ_0, given in Table 1. Unfortunately at μ_0, precisely the region in which the threshold for the excitations of the vortex core are observed, the semiclassical approximation breaks down. Both components of the wave functions at μ_0, $f_\pm^e$, are given in Fig. 2 for $R = 0.4$ at $k_\perp = 50$. At yet higher angular momenta the wave function is concentrated far from the inclusion and energy approaches the universal envelop curve well described by Eq. (6) (see blue lines). For large $k_\perp$ the semiclassical spectrum becomes accurate before the approximation breaks down near $b = R$. Of course, the spectrum at small μ is different, even for R as small as 0.1ξ,

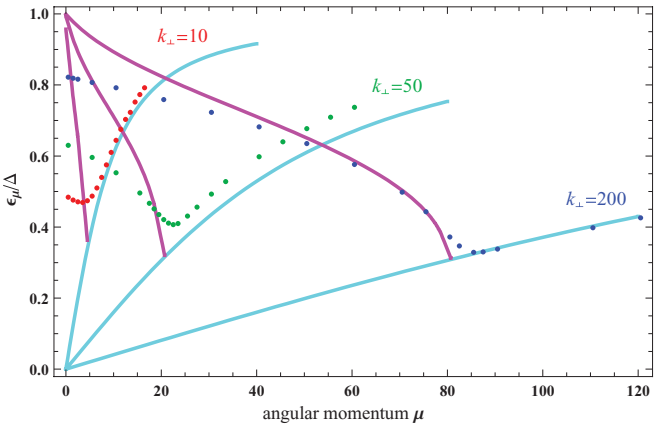

FIG. 1. (Color) Energy of quasiparticles for positive angular momenta for three values of $k_\perp$ for the hole radius $R = 0.4\xi$. Our numerical results are given by dots, while the semiclassical results and the perturbative results of Ref. 18 are given by purple (dash) and light blue (solid) lines respectively.

compared to the spectrum of the unpinned vortex[7] that is close to the $b > R$ semiclassical solution given by Eqs. (22), (27), and (30) of Ref. 18, plotted as a blue line in Fig. 1.

According to Refs. 5 and 18 the results of quasiclassical theory are valid under conditions, $k_\perp \xi \gg 1$ while perturbation

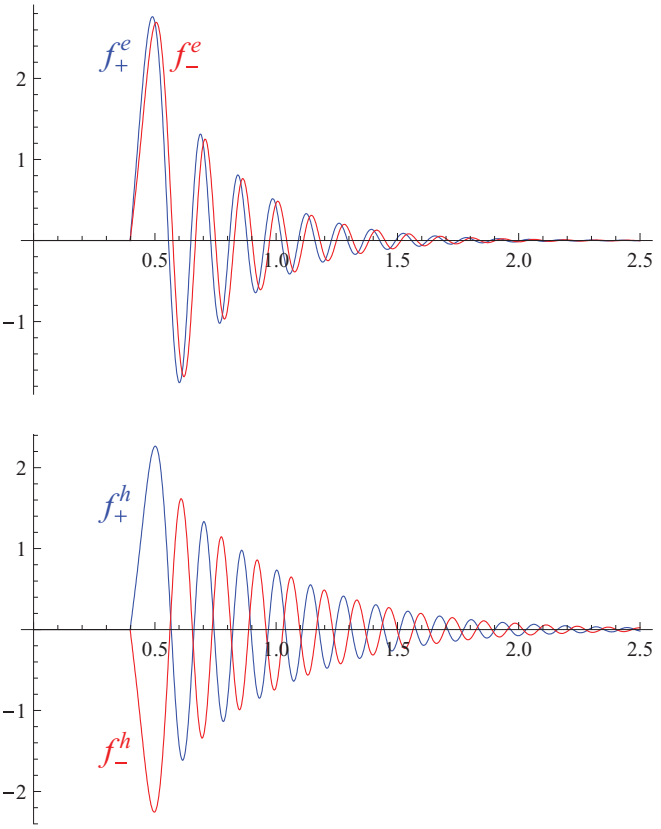

FIG. 2. (Color) Components of the eigenvectors of the BdG equations for $R = 0.4\xi$, $k_\perp \xi = 50$ at angular momentum μ_0 as functions of the distance from the center of inclusion (in units of ξ). Quasiparticles (upper plot) and quasiholes (lower plot) differ by the sign of the lower component of the spinor.

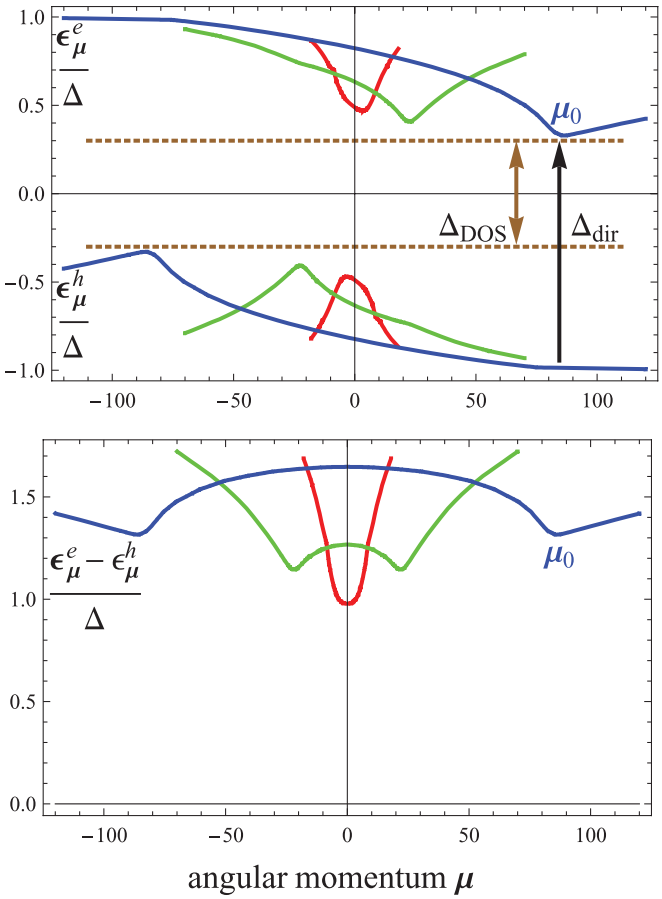

FIG. 3. (Color) Full spectrum of Andreev bound states and transitions between them (top plot). While the minigap seen by STM, Δ_{DOS} is between a quasiparticle state with angular momentum $\mu^e = \mu_0$ and quasihole with $\mu^h = -\mu_0$ (brown arrow), the microwave absorption gap, Δ_{dir}, is between the states with $\mu^e = \mu_0 = \mu^h - 1$ (brown arrow) and shown on the bottom plot. Clearly $\Delta_{dir} > \Delta_{DOS}$.

theory hinges on an additional condition $\mu/k_\perp R > 1$. Clearly our results agree with the quasiclassical approach better for large $k_\perp$ (see Fig. 1).

To calculate the microwave absorption across the minigap, one needs also the negative energy states as well as negative μ. According to the symmetry [Eq. (7)], it is sufficient to calculate the $\mu > 0$ quasihole states. The whole spectrum is shown in Fig. 3 for $R = 0.4$. Red, green and blue curves denote $k_\perp = 10, 50, 200$, respectively. It demonstrates that due to the lack of $\mu \to -\mu$ symmetry the minimal gap occurs between a particle with μ_0 and a hole with $-\mu_0$. It is important to note that μ_0 grows monotonically as $k_\perp$ increases, see the fifth column in Table I.

The minimal gap $\Delta_{DOS} = 2E_{\mu_0,k_\perp^{max}}$ (see arrows) can be measured by STM from the expression for tunneling differential conductance,

$$\frac{dI}{dV} = \left(\frac{dI}{dV}\right)_N \int_{-\infty}^{\infty} \frac{N(r,E)}{N_0} \frac{\partial f_F(E-eV)}{\partial V} dE, \quad (11)$$

TABLE I. The tunneling and microwave minigaps.

$k_\perp\xi$	R/ξ	μ_0	I_{μ_0}	Δ_{dir}/Δ	Δ_{DOS}/Δ
10	0.1	1.5	8.27	0.51	0.5
10	0.4	3.5	7.58	0.96	0.93
10	0.8	6.5	7.71	1.42	1.37
50	0.1	7.5	40.79	0.76	0.39
50	0.4	22.5	45.22	1.1	0.88
50	0.8	42.5	47.44	1.47	1.25
200	0.1	24.5	—	1.04	0.2
200	0.4	73.5	—	1.26	0.71

where f_F is the Fermi function, I and V are the current and applied voltage, correspondingly, and the local density of states below threshold is

$$N(r,E) = \sum_{\mu,k_\perp} |f^+_{k_\perp,\mu}|^2 \delta(E - E_{k_\perp,\mu}) + |f^-_{k_\perp,\mu}|^2 \delta(E + E_{k_\perp,\mu}). \quad (12)$$

This gap does not correspond to the direct transitions in microwave experiments with angular momenta $\mu^e - \mu^h = \pm 1$. In Fig. 3 the direct minigap Δ_{dir} as a function of the angular momentum is shown. The minimum appears at μ_0. The tunneling density of states exhibiting the smaller minigap Δ is determined directly by the eigenfunctions of the quasiparticle excitations (shown in Fig. 2) and the quasihole excitations as in Ref. 5. On the contrary the microwave response depends also on the dipole matrix elements leading to the selection rules.

IV. MICROWAVE ABSORPTION DUE TO CORE STATES

In the presence of the magnetic field the direct energy minigap Δ_{dir} should be observable in microwave absorption.[21] The calculation of the energy absorption[22] in one vortex is very similar to that of the interband transition in a cylindrically symmetric quantum dot.[23] In the present case at zero temperature the hole branch is occupied, while the electron branch is empty. Coupling of time-dependent external field $\mathbf{A}_{mw}$ (assumed to be a plane wave propagating parallel to the z axis in the gauge $\nabla \cdot \mathbf{A}_{mw} = 0$) in linear response is described by the operator [returning to physical units and with momentum operator defined in Eq. (2)]:

$$V = -\frac{e}{mc} \begin{pmatrix} \mathbf{A}_{mw} \cdot \Pi & 0 \\ 0 & -\mathbf{A}_{mw} \cdot \Pi \end{pmatrix}. \quad (13)$$

In the dipole approximation, the real part of the AC conductivity for the left-handed circular polarization $\mathbf{E}_{mw} = E_0(\cos(\omega t), \sin(\omega t))$ is

$$\sigma(\omega) = \frac{2\pi e^2}{m^2\omega} \rho \sum_{\mu,\mu',k_z} |M_{\mu\mu' k_z}|^2 \delta\left(E^e_{\mu k_z} - E^h_{\mu' k_z} - \hbar\omega\right). \quad (14)$$

The density of vortex lines can be written, using the flux quantization, as $\rho = B/\Phi_0$. The transition amplitudes are

$$\begin{aligned} M_{\mu\mu' k_z} &= \int d^2 r \left(u^{e*}_{\mu' k'_z} \; v^{e*}_{\mu' k'_z} \right) \begin{pmatrix} \Pi^x + i\Pi^y & 0 \\ 0 & -\Pi^x - i\Pi^y \end{pmatrix} \begin{pmatrix} u^h_{\mu k_z} \\ v^h_{\mu k_z} \end{pmatrix} \\ &= 2\pi^2 \hbar^2 i \delta_{\mu-\mu'-1} I_\mu \\ I_\mu &= \int dr \; r \left\{ f^{e-}_{\mu-1} \left(\frac{\mu+1}{r} + \partial_r \right) f^{h-}_{\mu} \right. \\ &\quad \left. - f^{e+}_{\mu-1} \left(\frac{\mu}{r} + \partial_r \right) f^{h+}_{\mu} \right\}. \end{aligned} \tag{15}$$

As expected, the angular momentum of the states in the quasiparticle and quasihole bands differ by 1. The matrix element at $\mu_0(k_\perp)$ was calculated numerically and the results are given in Table I for various parameters.

One observes that the matrix element at the threshold increases linearly with $k_\perp$ and consequently the absorption is dominated by $k_\perp^{\max}$, therefore $\Delta_{\rm dir} = E_{\mu_0, k_\perp^{\max}} - E_{\mu_0 - 1, k_\perp^{\max}}$. Note that dependence of the matrix element of the dielectric inclusion radius is insignificant. Next we discuss the application to certain realistic systems.

V. DISCUSSION AND SUMMARY

To exemplify possible signatures of the "large" minigaps $\Delta_{\rm DOS}$ and $\Delta_{\rm dir}$, we consider two extreme realizations of the "clean" superconducting thin film. The first is $L_z = 10$ nm thick Pb film for which $T_c = 7.15$ K, $\xi = 50$ nm, $E_F = 9.5$ eV. The states on the Fermi surface (considered isotropic) obey

$$E_F = \frac{\pi^2 \hbar^2}{2 m_c^* L_z^2} n_z^2 + \frac{k_\perp^2 \hbar^2}{2m}, \tag{16}$$

where the integer n_z can take values from 1 to $L_z k_F/\pi = 50$. Correspondingly, the in-plane component of the momentum varies from zero to $\xi k_\perp = 790$. The second is the optimally doped $YBCO$ with $T_c = 93$ K, $\xi = 2.5$ nm, $m_c^* = 7 m_e$. The d-wave nature of pairing in high T_c cuprite has a certain effect on Andreev bound states that has been studied intensively for unpinned vortices and vortices pinned on metallic inclusions. The absorption threshold, in principle sharp, is smeared due to the d-wave nature of the energy gap. The effect of nodal quasiparticles is strongly suppressed by the limited phase space (measure zero) of the nodes.[12,20] The vortex structure prevents quasiparticles from approaching the nodes. When insulator inclusions are present the situation does not change in this respect. One therefore can use the s-wave results with a small value of $E_F = 0.3$ eV. For a film of thickness $L_z = 5$ nm only 10 levels $n_z = 1, \ldots, 10$ contribute. The highest values of $k_\perp$ are consequently very small $\xi k_\perp < 8$. The tunneling and microwave (or direct) minigap will result in appearance of absorption at $\Delta_{\rm DOS}$ and $\Delta_{\rm dir}$, given in Table I.

To summarize, the spectrum of the Andreev bound states, localized by the Abrikosov vortex pinned by the insulator inclusion (or nanohole) of the size of the coherence length, was studied theoretically. We show that in this case the BdG spectrum dramatically changes in comparison with that inside an unpinned Abrikosov vortex. While for the unpinned vortex (or the one pinned by a slight inhomogeneity or a normal metal inclusion) the spectrum is monotonic in the angular momentum μ, with lowest excitation at $\mu = 1/2$ of order Δ^2/E_F, in the case of the dielectric inclusion of a nanosize R, the low angular momenta excitations are pushed up toward the threshold Δ (gap of the superconductor) since the dielectric prevents electron orbits of radius R. As the angular momentum increases, the excitation energy decreases to a minimum given by Eq. (4) (see Figs. 2 and 3), and then rises approaching the threshold Δ at large angular momenta, very much like in an unpinned vortex. For Fermi energies large compared to Δ (we have considered E_F/Δ up to 500) the minimal excitation energy is $\Delta^{3/2}/{E_F}^{1/2} \gg \Delta^2/E_F$. Dependence on the radius of the insulator inclusion was also studied. Due to the approximate electron-hole symmetry, the lowest energy gap exists for the largest possible $k_\perp$.

The reconstruction of the quasiparticle excitations' spectrum has a significant impact on optical, transport, and thermodynamic properties of the superconductor under magnetic field. The excitation with minimal energy manifests itself in optical response. Generally, unpinned or pinned by metallic inclusion vortices lead to excitations in the microwave range of the spectrum. On the other hand, on the basis of the above estimate, when all the vortices are pinned by dielectric inclusions or holes, the absorption spectrum should move to the infrared range. One therefore is led to conclude that the sample with nanoholes (like the one used recently to study insulator-superconductor transition[24]) becomes "transparent" to the microwave pulse.[21] Similarly, dissipation in the vortex system at sufficiently high frequencies, due to "vortex viscosity" closely associated with the quasiparticle excitations, is greatly reduced.

We speculate that the spectrum reconstruction also plays a role in transport phenomena broadly associated with the "superconductor-insulator" transition[25] in quasi-two-dimensional systems. In these materials small insulating inclusions (islands) are generally present and, since the width is small, can be considered as "columnar." In that case our results are applicable. Experimentally magnetoresistance first rises dramatically as the magnetic field is increased and subsequently decreases.[25] It has been established that the long-range superconducting correlations are suppressed so there is no supercurrent contribution to conductivity. As a result transport is dominated by the normal component. Why does this normal component of the conductivity become so small? It might be that the normal excitations are suppressed by the spectrum reconstruction due to pinning on insulator inclusions. At very high magnetic fields not all the vortices are pinned and the normal component is no longer suppressed.

ACKNOWLEDGMENTS

We acknowledge support from the Israel Scientific Foundation (Grant No. 499/07). Work of B.R. was supported by the MOE ATU program, National Science Council of R.O.C. Grants No. 99-2112-M-009- 014-MY3, and acknowledges the hospitality and support at Physics Department of Bar Ilan University.

[1]P. W. Anderson, *Basic Notions of Condensed Matter Physics* (Benjamin-Kummings, London, 1984).
[2]R. E. Glover and M. Tinkham, Phys. Rev. **108**, 243 (1957).
[3]D. C. Mattis and J. Bardeen, Phys. Rev. **111**, 412 (1958).
[4]I. Giaever, Phys. Rev. Lett. **5**, 147 (1960).
[5]J. B. Ketterson and S. N. Song, *Superconductivity* (Cambridge University Press, New York, 1999).
[6]C. Caroli, P. G. de Gennes, and J. Matricon, Phys. Lett. **9**, 307 (1964).
[7]W. L. Clinton, Phys. Rev. B **46**, 5742 (1992).
[8]P. G. deGennes, *Superconductivity of Metals and Alloys* (W. A. Benjamin, New York, 1966).
[9]J. Bardeen, R. Kümmel, A. J. Jacobs, and L. Tewordt, Phys. Rev. **187**, 556 (1969).
[10]F. Gygi and M. Schlüter, Phys. Rev. B **41**, 822 (1990); **43**, 7609 (1991).
[11]J. D. Shore, M. Huang, A. T. Dorsey, and J. P. Sethna, Phys. Rev. Lett. **62**, 3089 (1989); C. Berthod, Phys. Rev. B **71**, 134513 (2005).
[12]N. Schopohl and K. Maki, Phys. Rev. B **52**, 490 (1995); I. Knezevic and Z. Radovic, Physica C **317**, 640 (1999); D. Rainer, J. A. Sauls, and D. Waxman, Phys. Rev. B **54**, 10094 (1996).
[13]H. F. Hess, R. B. Robinson, R. C. Dynes, J. M. Valles, and J. V. Waszczak, Phys. Rev. Lett. **62**, 214 (1989).
[14]L. Shan *et al*., Nat. Phys. **7**, 325 (2011).
[15]A. Tonomura *et. al*., Nature (London) **412**, 629 (2001).
[16]V. Metlushko, U. Welp, G. W. Crabtree, Z. Zhang, S. R. J. Brueck, B. Watkins, L. E. DeLong, B. Ilic, K. Chung, and P. J. Hesketh, Phys. Rev. B **59**, 603 (1999); P. Vavassori, V. Metlushko, M. Grimsditch, B. Ilic, P. Neuzil, and R. Kumar, *ibid*. **61**, 5895 (2000); A. Yu. Aladyshkin1 *et al*., Supercond. Sci. Technol. **22**, 053001 (2009) and references therein; V. R. Misko, D. Bothner, M. Kemmler, R. Kleiner, D. Koelle, F. M. Peeters, and F. Nori, Phys. Rev. B **82**, 184512 (2010); R. Wördenweber, P. Dymashevski, and V. R. Misko, *ibid*. **69**, 184504 (2004); M. Kemmler, C. Gürlich, A. Sterck, H. Pöhler, M. Neuhaus, M. Siegel, R. Kleiner, and D. Koelle, Phys. Rev. Lett. **97**, 147003 (2006).
[17]J. C. Keay, P. R. Larson, K. L. Hobbs, M. B. Johnson, J. R. Kirtley, O. M. Auslaender, and K. A. Moler, Phys. Rev. B **80**, 165421 (2009); I. Sochnikov *et al*., Nature Nanotechnology **5**, 516 (2010).
[18]A. S. Mel'nikov, A. V. Samokhvalov, and M. N. Zubarev, Phys. Rev. B **79**, 134529 (2009).
[19]N. B. Kopnin, A. S. Mel'nikov, V. I. Pozdnyakova, D. A. Ryzhov, I. A. Shereshevskii, and V. M. Vinokur, Phys. Rev. B **75**, 024514 (2007).
[20]G. E. Volovik, Pisma Zh. Eksp. Teor. Fiz. **57**, 233 (1993) [JETP Lett. **57**, 244 (1993)].
[21]K. Steinberg, M. Scheffler, and M. Dressel, Phys. Rev. B **77**, 214517 (2008).
[22]B. Janko and J. D. Shore, Phys. Rev. B **46**, 9270 (1992).
[23]J. H. Davies, *The Physics of Low-Dimensional Semiconductors* (Cambridge University Press, New York, 1998).
[24]M. D. Stewart *et al*., Science **318**, 1273 (2007); H. Q. Nguyen, S. M. Hollen, M. D. Stewart, J. Shainline, A. Yin, J. M. Xu, and J. M. Valles, Phys. Rev. Lett. **103**, 157001 (2009).
[25]V. F. Gantmakher and V. T. Dolgopolov, Phys. Usp. **53**, 1 (2010) and references therein.